Robustness of narrowband DOA algorithms with respect to signal bandwidth

Jean-Pierre Delmas, Yann Meurisse

Robustness of narrowband DOA algorithms with respect to signal bandwidth

Jean-Pierre Delmas, Yann Meurisse

October 24, 2021

Paper 4487 submitted to Signal Processing

Département CITI, Institut National des Télécommunications, 9 rue Charles Fourier, 91011 Evry Cedex, FRANCE.

Fax: +33-1-60 76 44 33, e-mail: jean-pierre.delmas@int-evry.fr.

Keywords: direction of arrival estimation, narrowband source location algorithm, wideband source location algorithm, nonzero bandwidth, offset frequency

Abstract

The purpose of this paper is to determine the domain of validity of spatial covariance-based narrowband DOA algorithms when processing non-narrowband data. By focusing on the case of one source and two equipowered uncorrelated sources of the same bandwidth, we examine order detection and asymptotic bias and covariance w.r.t. the bandwidth and the number of snapshots given by any narrowband algorithm. An order detector scheme, based on numerical analysis arguments introduced in channel order detection, is proposed. Closed-form expressions are given for the asymptotic bias and covariance of the DOA's estimated by the MUSIC algorithm, for which we show the key role that bandwidth plays w.r.t. the demodulation frequency. Furthermore, a common closed-form expression of the Cramer-Rao bound is given for the DOA parameter of a narrowband or wideband source, whose spectrum is symmetric w.r.t. the demodulation frequency, in the case of an arbitrary array. This allows us to prove that the MUSIC algorithm retains its efficiency over a large bandwidth range under these conditions.

1 Introduction

The problem of estimating the directions of arrival (DOA) of multiple plane waves impinging on an array of sensors may be classified into narrowband and wideband data processing, according to whether the complex envelope of the received signals can be considered as constant versus variable in time along the array. As the wideband approaches generally require an increased computational complexity (see e.g., [12] and the references therein) compared to the narrowband ones, it is of interest to examine if the narrowband methods can be used for a sufficiently wide bandwidth without sacrificing performance. This question, interestingly, has received little attention in the literature. Schell and Gardner [17] mention the breakdown of narrowband approximations as one departure from ideality among potentially others. Several authors have proposed definitions of the narrowband scenario but have not related it to the performance of DOA algorithms. Based on the result shown in [4] that more than 99.99% of the received power from a single signal is characterized by the $r = \lceil 2b\tau_\theta + 1 \rceil$ largest eigenvalues of the spatio-temporal covariance matrix (where b is the bandwidth of the received signal and τ_θ is the propagation time across the array including time spent traveling through the delay lines in the sensors), Buckley [4] defined as a narrowband scenario the case where $2b\tau_\theta + 1$ is sufficiently close to one. For wider bandwidths and greater propagation time across the array, this notion of effective rank allows Buckley and Griffiths [5] to propose a signal subspace algorithm in the

context of wideband signals. A similar approach has been proposed in the context of spatial signal processing in [22] in which a signal is considered narrowband if the second eigenvalue of the signal's noise-free spatial covariance matrix is smaller than the noise power. And recently, the effect of nonzero bandwidth which is symmetric spectra w.r.t. the demodulation frequency of the estimated DOA's has been analyzed in [18].

The purpose of this work is twofold. First, we extend the analysis of [18] to the case of nonsymmetric spectra and/or offset of the centered value of the spectra w.r.t. the demodulation frequency. Second, considering order detection, the Cramer-Rao bound and the comparison between narrowband and wideband algorithms, we prove that the vague definition of a narrowband scenario often given in the literature, namely, that the array aperture is much less than the inverse relative bandwidth (i.e., $\frac{Mb}{f_0} \ll 1$ where M denotes the number of sensors and where the spacing between sensors is the halfwavelength) is far too severe in the cases of one source or of two equipowered uncorrelated sources of the same bandwidth.

This paper is organized as follows. After the data model and some notations are introduced in Section 2, the performance of the eigendecomposition-based order detectors are considered, where a criterion based on numerical analysis arguments [13] is proposed in Section 3. The asymptotic bias and covariance (w.r.t. the number of snapshots and the signal bandwidth) of the estimated DOA's are then studied and illustrated in the case of the standard MUSIC algorithm in Section 4. A common closed-form expression of the Cramer-Rao bound (CRB) is given for the DOA parameter of a narrowband or wideband single source of any power spectral density symmetric w.r.t. the demodulation frequency in the case of an arbitrary array in Section 5. Finally, Section 6 is devoted to comparisons between narrowband and wideband algorithms for two scenarios.

The following notations are used throughout the paper. Matrices and vectors are represented by bold upper case and bold lower case characters, respectively. Vectors are by default in column orientation, while T, H and $*$ stand for transpose, conjugate transpose, conjugate, respectively. $\mathrm{E}(\cdot)$, $\mathrm{Cov}(\cdot)$ and $\mathrm{Tr}(\cdot)$ denote the expectation, the covariance and the trace, respectively. Vec(.) is the "vectorization" operator that rearranges a matrix into a vector consisting of the columns of the matrix stacked one below another; it will be used in conjunction with the Kronecker product $\mathbf{A} \otimes \mathbf{B}$ as the block matrix whose (i, j) block element is $a_{i,j}\mathbf{B}$. The symbol $\odot$ denotes elementwise multiplication of $\mathbf{A}$ and $\mathbf{B}$ ($[\mathbf{A} \odot \mathbf{B}]_{i,j} = \mathbf{A}_{i,j}\mathbf{B}_{i,j}$). $\mathrm{Diag}(a_1, \ldots, a_n)$ is a diagonal matrix with diagonal elements a_i and $\mathbf{1}$ is the vector of all ones, whose dimension is inferred from the context.

2 Data model

Consider K radiating sources impinging on an arbitrary array of M sensors. The received signals that are assumed wide-sense stationary, are bandpass filtered [1] (with bandwidth B) around the frequency f_0 of interest (with $B < 2f_0$, see e.g., [11, Section 15.3]). After down-shifting the sensor signals to baseband, the complex envelope is generated. If the background noise is white, the continuous-time noise envelope is white in the bandwidth $[-\frac{B}{2}, +\frac{B}{2}]$. After sampling the complex envelope signals at the rate $\frac{1}{T_s} \ll B$, the M-vectors of observed complex envelope at the array output at times $t = 1, \ldots, T$ form independent snapshots. The M-vector $\mathbf{n}_t$, containing the complex envelope of the noise, is assumed throughout the paper to be temporally and spatially uncorrelated, with $\mathrm{E}(\mathbf{n}_t \mathbf{n}_t^H) = \sigma_n^2 \mathbf{I}_M$, and independent of the sources. If s_t^k denotes the complex envelope of the kth source w.r.t. the frequency f_0 of interest and $\mu_k(f)$ its spectral measure [6, chap. 3] [2], the complex envelope of this source observed at the mth sensor is $s_{t-\tau_{k,m}}^k e^{-i2\pi f_0 \tau_{k,m}}$, where $\tau_{k,m}$ is the propagation delay associated with the kth source and the mth sensor. These delays $\tau_{k,m}$ contain information about the kth DOA θ_k [3], and we set $\Theta \stackrel{\text{def}}{=} (\theta_1, \ldots \theta_K)^T$. The M-vector of observed complex envelope at the array output is then

$$\mathbf{y}_t = \sum_{k=1}^{K} \int_{-B/2}^{+B/2} e^{i2\pi f t} \mathbf{a}(\theta_k, f_0 + f) d\mu_k(f) + \mathbf{n}_t,$$

where $\mathbf{a}(\theta_k, \nu) \stackrel{\text{def}}{=} [e^{-i2\pi\nu\tau_{k,1}}, \ldots, e^{-i2\pi\nu\tau_{k,M}}]^T$. If the sources are spatially uncorrelated, the spatial covariance matrix may be written as

$$\mathbf{R}_b = \mathrm{E}(\mathbf{y}_t \mathbf{y}_t^H) = \sum_{k=1}^{K} \int_{-B/2}^{+B/2} S_k(f) \mathbf{a}(\theta_k, f_0 + f) \mathbf{a}^H(\theta_k, f_0 + f) df + \sigma_n^2 \mathbf{I}_M, \tag{2.1}$$

where $S_k(f)$ denotes the power spectral density of the kth source. For the zero bandwidth case, this matrix becomes:

$$\mathbf{R}_0 = \sum_{k=1}^{K} \sigma_k^2 \mathbf{a}(\theta_k, f_0) \mathbf{a}^H(\theta_k, f_0) + \sigma_n^2 \mathbf{I}_M, \tag{2.2}$$

where σ_k^2 denotes the power of the kth source. We consider that the power spectral density $S_k(f)$ of the complex envelope of the kth wideband source is parameterized by its centered frequency $f_m \stackrel{\text{def}}{=} \frac{\int f S_k(f) df}{\int S_k(f) df}$, its standard

[1] We suppose that their power spectral densities are zero near DC.

[2] This spectral representation $s_t^k = \int_{-B/2}^{+B/2} e^{i2\pi f t} d\mu_k(f)$ enables us to easily generate wide-sense stationary bandlimited processes by the approximation: $s_t^k \approx \sum_{l=0}^{L-1} a_l^k e^{i2\pi f_l t}$ with $f_l \stackrel{\text{def}}{=} \frac{-L+2l+1}{2L} B$, $L \gg 1$ (with $L = 200$ in Monte Carlo simulations) and $(a_l^k)_{l=0,\ldots,L-1, k=1,\ldots,K}$ are uncorrelated random variables with $\mathrm{E}|a_l^k|^2 = \frac{B}{L} S_k(f_l)$, where $S_k(f)$ denotes the power spectral density of s_t^k.

[3] For notational simplicity we assume that θ_k is a real scalar.

deviation $f_\sigma \stackrel{\text{def}}{=} \left(\frac{\int (f-f_m)^2 S_k(f) df}{\int S_k(f) df}\right)^{\frac{1}{2}}$ [4] and by its power σ_k^2. The kth source spectrum is expressed by $S_k(f) = \frac{\sigma_k^2}{f_\sigma} S\left(\frac{f-f_m}{f_\sigma}\right)$, if $S(f)$ denotes a normalized function, i.e. a function satisfying

$$\int S(f)df = 1, \quad \int fS(f)df = 0, \quad \text{and} \quad \int f^2 S(f)df = 1, \tag{2.3}$$

and the k-th source correlation is $R_k(t) = \sigma_k^2 R(f_\sigma t) e^{i2\pi f_m t}$ where $R(t)$ denotes the correlation function associated with $S(f)$ which satisfies from (2.3)

$$R(0) = 1 \quad , \quad R'(0) = 0 \quad , \quad R''(0) = -4\pi^2.$$

Because $\mathbf{a}(\theta_k, f_0 + f)\mathbf{a}^H(\theta_k, f_0 + f) = \mathbf{a}(\theta_k, f_0)\mathbf{a}^H(\theta_k, f_0) \odot \mathbf{a}(\theta_k, f)\mathbf{a}^H(\theta_k, f)$, the covariance matrix $\mathbf{R}_b$ may be written as

$$\mathbf{R}_b = \sum_{k=1}^{K} \mathbf{a}(\theta_k, f_0)\mathbf{a}^H(\theta_k, f_0) \odot \mathbf{R}_{s_k} + \sigma_n^2 \mathbf{I}_M, \tag{2.4}$$

where $\mathbf{R}_{s_k}$ is the $M \times M$ matrix whose (m,n)th term is the source correlation

$$\begin{aligned} [\mathbf{R}_{s_k}]_{m,n} = \mathrm{E}(s^k_{t-\tau_{k,m}} {s^k_{t-\tau_{k,n}}}^*) &= \int_{-B/2}^{+B/2} S_k(f) e^{i2\pi f(\tau_{k,n}-\tau_{k,m})} df = \sigma_k^2 \int S(\nu) e^{i2\pi(\nu f_\sigma + f_m)(\tau_{k,n}-\tau_{k,m})} d\nu \\ &= \sigma_k^2 R\left(f_\sigma(\tau_{k,n}-\tau_{k,m})\right) e^{i2\pi f_m(\tau_{k,n}-\tau_{k,m})}. \end{aligned} \tag{2.5}$$

If $\mathbf{z}_m$ and $\mathbf{p}_k$ denote, respectively, the coordinate vector of the mth sensor referenced to a specific sensor and the unit wavevector associated with the kth source, then $\tau_{k,m} = \frac{1}{f_0}\frac{\mathbf{z}_m^T \mathbf{p}_k}{\lambda_0}$ (e.g., for a linear array, $\tau_{k,m} = \frac{d_m}{c}\sin\theta_k = \frac{1}{f_0}\frac{d_m}{\lambda_0}\sin\theta_k$ where θ_k is the kth DOA relative to the array broadside, c is the propagation velocity, d_m is the distance from sensor m to a reference sensor and $\lambda_0 \stackrel{\text{def}}{=} \frac{c}{f_0}$). Because $\mathbf{R}_{s_k} = \sigma_k^2 \mathbf{1}\mathbf{1}^T$ in the zero bandwidth case, we prove in Appendix A that $\mathbf{R}_{s_k} = \sigma_k^2 \mathbf{1}\mathbf{1}^T + \delta\mathbf{R}_{s_k}$ with

$$[\delta\mathbf{R}_{s_k}]_{m,n} = \sigma_k^2 \alpha_{m,n,k}\left[i2\pi\left(\frac{f_m}{f_0}\right) - 2\pi^2 \alpha_{m,n,k}\left(\frac{f_\sigma^2}{f_0^2}\right)\right] + O\left(\frac{f_m^2}{f_0^2}\right) + O\left(\frac{f_\sigma^3}{f_0^3}\right) + O\left(\frac{f_m f_\sigma^2}{f_0^3}\right) \tag{2.6}$$

for an arbitrary spectrum

$$= -2\pi^2 \sigma_k^2 \alpha_{m,n,k}^2 \left(\frac{f_\sigma^2}{f_0^2}\right) + O\left(\frac{f_\sigma^3}{f_0^3}\right) \quad \text{for an arbitrary spectrum centered at } f_0, \tag{2.7}$$

$$= -2\pi^2 \sigma_k^2 \alpha_{m,n,k}^2 \left(\frac{f_\sigma^2}{f_0^2}\right) + O\left(\frac{f_\sigma^4}{f_0^4}\right) \quad \text{for a symmetric spectrum centered at } f_0, \tag{2.8}$$

with $\alpha_{m,n,k} \stackrel{\text{def}}{=} \frac{(\mathbf{z}_n - \mathbf{z}_m)^T \mathbf{p}_k}{\lambda_0}$. Therefore $\mathbf{R}_b$ may be considered as a perturbation of $\mathbf{R}_0$:

$$\mathbf{R}_b = \mathbf{R}_0 + \delta\mathbf{R}_b \qquad \text{with} \qquad \delta\mathbf{R}_b = \sum_{k=1}^{K} \mathbf{a}(\theta_k, f_0)\mathbf{a}^H(\theta_k, f_0) \odot \delta\mathbf{R}_{s_k} \tag{2.9}$$

[4] In the special case of sources with uniform spectrum in $[f_0 - \frac{b}{2}, f_0 + \frac{b}{2}]$, $f_m = 0$ and $f_\sigma = \frac{b}{2\sqrt{3}}$.

3 Performance of the detector

First, we consider the performance of the eigendecomposition-based order detectors. Many methods have been suggested for the detection of the number of sources in array processing. The most commonly used detectors are formulated in terms of the eigenvalues of the sample spatial covariance matrix $\mathbf{R}_b(T)$ derived from T independent snapshots $\mathbf{y}_t$. Typical examples are the Akaike information criterion (AIC) and the minimum description length (MDL) detectors. These methods are easy to implement and as long as the data come from the idealized zero bandwidth assumption; MDL gives a strongly consistent estimate of the number of sources independent of the signal-noise-ratio. Unfortunately if the bandwidth of the signal increases, the AIC and MDL criteria rapidly tend to overestimate the number of sources and, in practice, the estimated number of sources by these detectors may be far from the true number [21]. The general design of robust detection methods that work with non-narrowband signal remains an open problem.

The detection of the number of non-narrowband signals from the sample spatial covariance matrix, however, is analogous to the detection of the "effective" order of the impulse response of a channel from the sample spatio-temporal covariance matrix. In fact, the sample spatial covariance matrix $\mathbf{R}_b(T)$ observed in a non-narrowband scenario can be considered as the sum of an "ideal" rank-K matrix $\mathbf{R}$ and a "perturbation" matrix $\delta\mathbf{R}_{b,T}$,

$$\mathbf{R}_b(T) = \mathbf{R} + \delta\mathbf{R}_{b,T}$$

where K is the number of sources and $\mathbf{R}$ is the signal's noise-free spatial covariance matrix associated with K zero bandwidth signals. The "perturbation" matrix $\delta\mathbf{R}_{b,T}$ incorporates the influence of the non-narrowband assumption, the influence of the additive noise, and the influence of the estimated (i.e., inexact) statistics. Using the concept of canonical angles between subspaces and invariant subspace perturbation results, a "maximally stable" decomposition of the range space of the sample covariance matrix into signal and noise subspace has been proposed in the channel order determination context by Liavas *et al.* [13]. This approach leads to the following criterion: The detected order $\widehat{K}$ is the value of k which minimizes

$$r(k) \stackrel{\text{def}}{=} \begin{cases} \frac{\lambda_{k+1}}{\lambda_k - 2\lambda_{k+1}}, & \text{if } \lambda_{k+1} \leq \frac{\lambda_k}{3} \\ 1, & \text{otherwise} \end{cases}$$

where $\lambda_1 \geq \lambda_2 \geq \ldots \geq \lambda_M$ denote the eigenvalues of the sample covariance matrix $\mathbf{R}_b(T)$. We propose applying this criterion in the context of non-narrowband array processing. Contrary to the AIC and MDL criteria, which base their detection on the similarity of the smallest eigenvalues, the proposed criterion is based on the existence

of an eigenvalue gap; these points are detailed in [14]. Because simulations (see, e.g., Fig.1 and [22]) show that as the signal's bandwidth is increased, eigenvalues pop up from the noise floor one at a time, the proposed criterion is potentially promising.

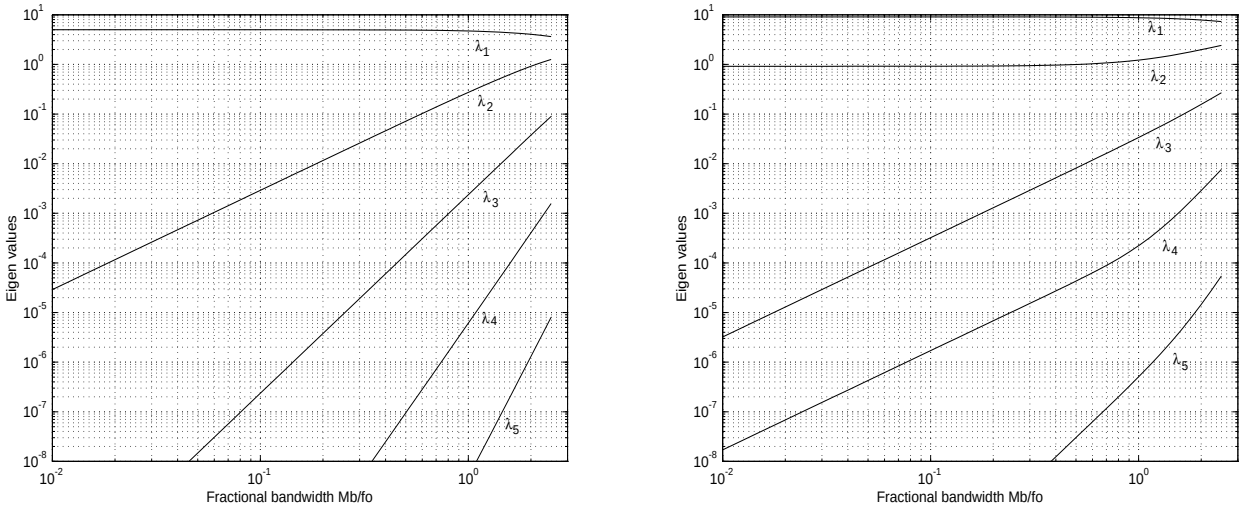

Fig.1 Eigenvalues of the signal's noise-free spatial covariance matrix for one or two equipowered sources (DOA separation of 15°) of centered flat spectrum of bandwidth b and a uniform linear array of $M = 5$ sensors as a function of the fractional bandwidth $\frac{Mb}{f_0}$.

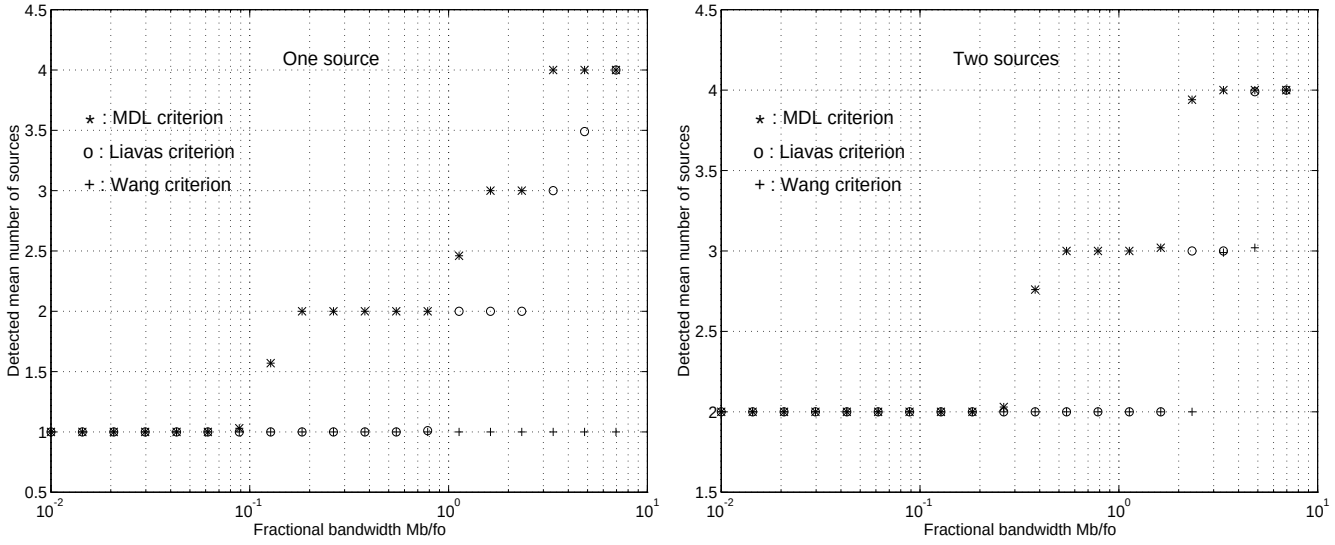

Fig.2 Detected mean number of sources (from 100 runs) by the MDL, Liavas and Wang criteria as a function of the fractional bandwidth $\frac{Mb}{f_0}$ for a uniform linear array of $M = 5$ sensors, one or two equipowered sources (DOA separation of 15°), of centered flat spectrum of bandwidth b with a SNR of $20dB$ and $T = 320$ snapshots (10 sections of 32 frequencies for the Wang criterion).

Fig.2 compares the MDL and Liavas criteria to that derived for wideband signals proposed by Wang and Kaveh [20] with the same data (complex envelopes sampled at the Nyquist rate $\frac{1}{T_s} = b$). The figure shows that the Liavas criterion is much more robust to bandwidth increases than the MDL criterion. Naturally, the Wang criterion which

is adapted to wideband scenarios outperforms our criterion. What can be said about the quality of the estimates obtained by our criterion is given by its behavior as the snapshot size increases to infinity. Figs.3 [5] and 4 show, respectively, for one and two equipowered sources, the domain of fractional bandwidth $\frac{Mb}{f_0}$ for which the MDL and Liavas criteria correctly detect the number of sources in the large-sample limit (i.e., with exact statistics). In these figures the Liavas criterion consistently outperforms the MDL criterion. Furthermore, they show that the robustness of the MDL and Liavas criteria to a bandwitdh increase can be reduced with an increase of SNR or DOA separation [6]. Of course, a fair and thorough comparison between the MDL and Liavas criteria would require a large quantity of scenarios (various arrays, DOA's, sources spectra and SNR). For example, an extensive study of scenarios of two equipowered symmetric spectra sources impinging on a uniform linear array shows sometimes that the Liavas criterion falsely detects 1 source for a small number of sensors, a favorable SNR and a small DOA separation while the MDL criterion correctly detects 2 sources; similar cases are observed for two sources with different powers.

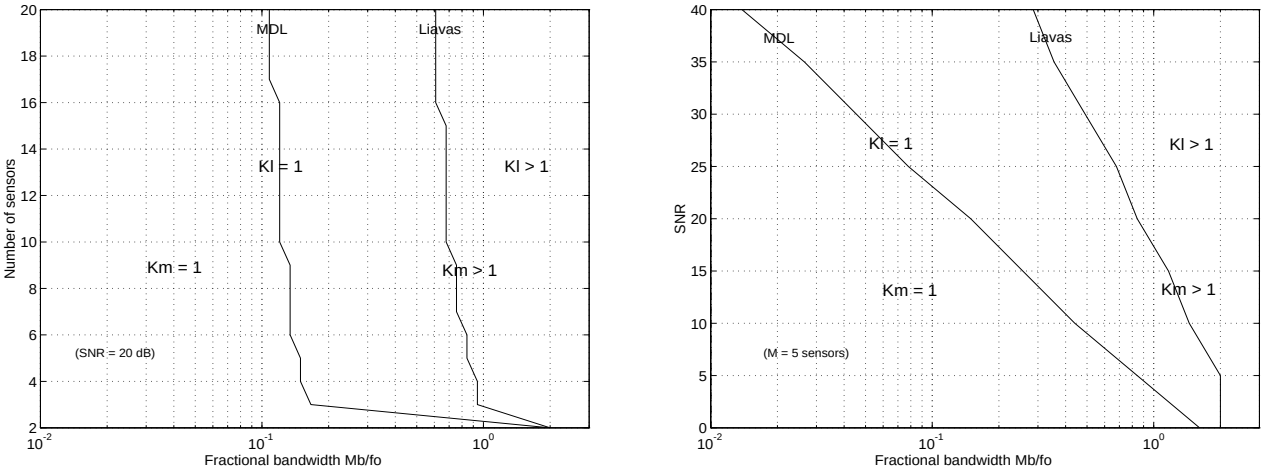

Fig.3 Asymptotic (w.r.t. the number of snapshots) detected number of sources by the MDL (Km) and Liavas (Kl) criteria as a function of the fractional bandwidth $\frac{Mb}{f_0}$, the number of sensors or the SNR for a uniform linear array and one source of centered flat spectrum of bandwidth b.

[5] For example, Fig.3a should be understood in the following way. The MDL criterion detects 1 source ($Km = 1$) for $\frac{Mb}{f_0}$ approximately less than 1.5×10^{-1} and otherwise more than 1 source, while the Liavas criterion detects 1 source ($Kl = 1$) for $\frac{Mb}{f_0}$ approximately less than 7×10^{-1} and otherwise more than 1 source.

[6] Because these detectors correctly detect the number of sources in the entire domain of SNR and DOA separation represented on these figures for zero bandwidth signals, this point does not contradict the improvement of the performance of these detector tests to increasing the SNR or DOA separation with narrowband signals.

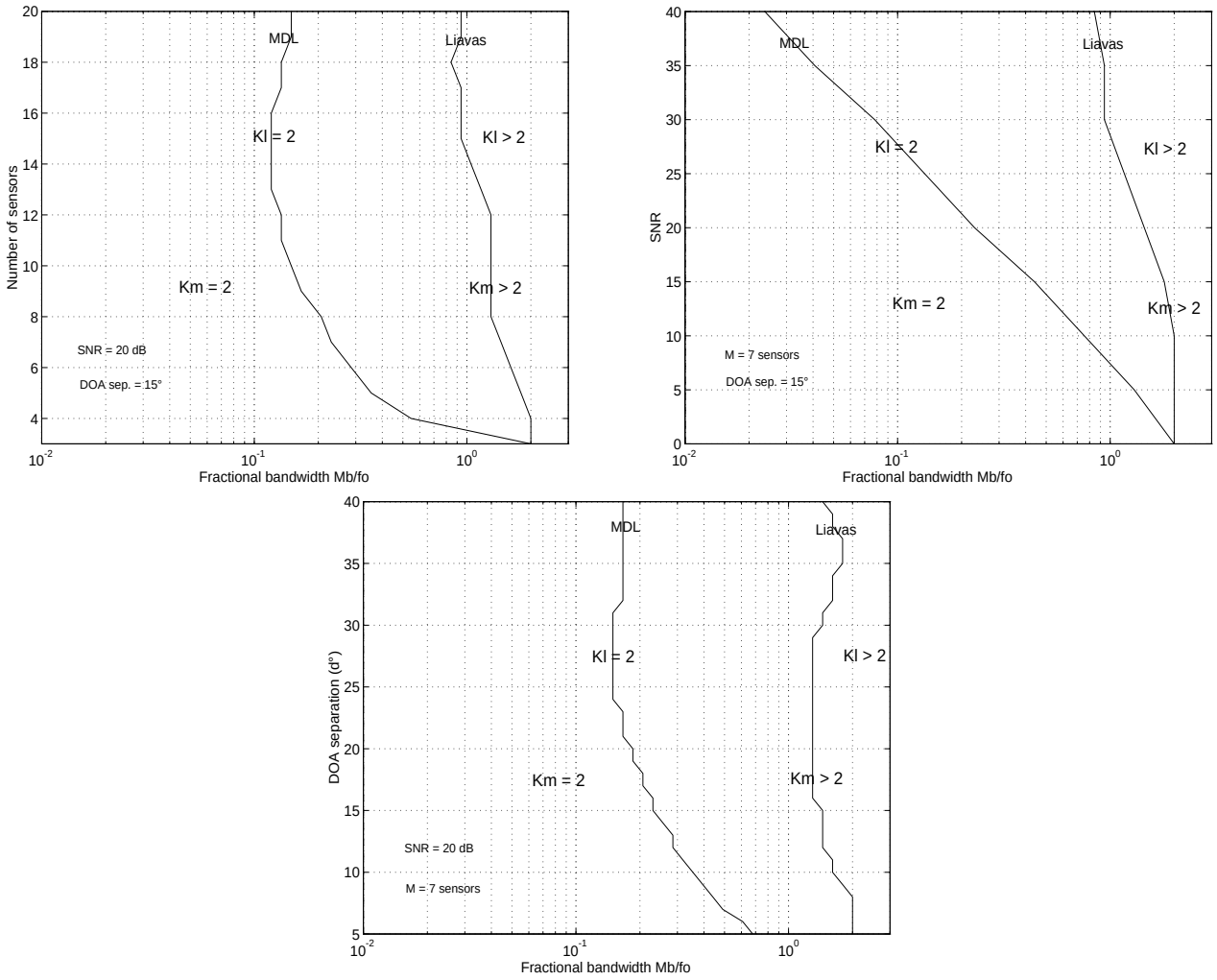

Fig.4 Asymptotic detected number of sources (w.r.t. the number of snapshots) by the MDL (Km) and Liavas (Kl) criteria as a function of the fractional bandwidth $\frac{Mb}{f_0}$, the number of sensors, the DOA separation or the SNR for a uniform linear array and two equipowered sources of centered flat spectrum of bandwidth b.

4 Asymptotic bias and covariance

To consider the asymptotic bias and covariance of the DOA's (w.r.t. to the number of snapshots and signal bandwidth) estimated by a narrowband second-order statistics (SOS)-based algorithm, we adopt a functional approach that consists of recognizing that the whole process of constructing an estimate $\Theta(T)$ of Θ is equivalent to defining a functional relation linking this estimate $\Theta(T)$ to the sample statistics $\mathbf{R}_b(T) = \frac{1}{T}\sum_{t=1}^{T} \mathbf{y}_t\mathbf{y}_t^H$ from which it is inferred. This functional dependence is denoted $\Theta(T) = \text{alg}(\mathbf{R}_b(T))$. Clearly, $\Theta = \text{alg}(\mathbf{R}_0)$, and therefore the different narrowband SOS-based algorithms alg$(\cdot)$ constitute distinct extensions of the mapping $\mathbf{R}_0 \rightarrow \Theta$ generated

by (2.2) to any unstructured Hermitian matrix $\mathbf{R}_b(T)$. $\mathbf{R}_b(T)$ may be considered as a perturbation of $\mathbf{R}_b$:

$$\mathbf{R}_b(T) = \mathbf{R}_b + \delta\mathbf{R}_T, \tag{4.1}$$

where $\delta\mathbf{R}_T$ is the finite sample size error, verifying $\mathrm{E}(\delta\mathbf{R}_T) = \mathbf{O}$ and $\mathrm{Cov}(\delta\mathbf{R}_T) = O\left(\frac{1}{T}\right)$. Because the mapping $\mathrm{alg}(\cdot)$ is sufficiently regular in a neighborhood of $\mathbf{R}_b$ for most SOS-based algorithms, we have from (4.1),

$$\Theta(T) = \mathrm{alg}(\mathbf{R}_b) + (D^{\mathrm{alg}}_{\mathbf{R}_b}, \delta\mathbf{R}_T) + O(\|\delta\mathbf{R}_T\|^2), \tag{4.2}$$

where $(D^{\mathrm{alg}}_{\mathbf{R}_b}, \delta\mathbf{R}_T)$ denotes the differential of the mapping $\mathrm{alg}(\cdot)$ evaluated at point $\mathbf{R}_b$ applied to $\delta\mathbf{R}_T$. Taking expectations, we obtain:

$$\mathrm{E}(\Theta(T)) = \mathrm{alg}(\mathbf{R}_b) + O\left(\frac{1}{T}\right). \tag{4.3}$$

By considering $\mathbf{R}_b$ as a perturbation of $\mathbf{R}_0$ (see (2.9)), a first-order perturbation analysis of a narrowband SOS-based algorithm acting on $\mathbf{R}_b$ evaluated at the point $\mathbf{R}_0$ gives

$$\begin{aligned} \mathrm{alg}(\mathbf{R}_b) &= \mathrm{alg}(\mathbf{R}_0) + (D^{\mathrm{alg}}_{\mathbf{R}_0}, \delta\mathbf{R}_b) + O(\|\delta\mathbf{R}_b\|^2) \\ &= \Theta + \mathbf{D}^{\mathrm{alg}}_{\mathbf{R}_0}\mathrm{Vec}(\delta\mathbf{R}_b) + O(\|\delta\mathbf{R}_b\|^2), \end{aligned} \tag{4.4}$$

where $\mathbf{D}^{\mathrm{alg}}_{\mathbf{R}_0}$ denotes the matrix associated with the differential [7] of the narrowband SOS-based algorithm $\mathrm{alg}(\cdot)$ at point $\mathbf{R}_0$. So, from (4.3),(4.4) and (2.9) and from (2.7) and (2.8) for spectra centered on f_0, the following result holds:

Result 1 *The asymptotic bias of the estimate $\Theta(T)$ (w.r.t. the number of snapshots and signal bandwidth) given by a narrowband SOS-based algorithm is given by:*

$$\begin{aligned} \mathrm{E}(\Theta(T)) - \Theta &= \mathbf{D}^{\mathrm{alg}}_{\mathbf{R}_0}\mathrm{Vec}(\delta\mathbf{R}_b) + O(\|\delta\mathbf{R}_b\|^2) + O\left(\frac{1}{T}\right) \quad \textit{for an arbitrary spectrum} \\ &= \sum_{k=1}^{K} \mathbf{b}^{\mathrm{alg}}_k \left(\frac{f_\sigma^2}{f_0^2}\right) + O\left(\frac{f_\sigma^3}{f_0^3}\right) + O\left(\frac{1}{T}\right) \quad \textit{for an arbitrary spectrum centered at } f_0 \qquad (4.5) \\ &= \sum_{k=1}^{K} \mathbf{b}^{\mathrm{alg}}_k \left(\frac{f_\sigma^2}{f_0^2}\right) + O\left(\frac{f_\sigma^4}{f_0^4}\right) + O\left(\frac{1}{T}\right) \quad \textit{for a symmetric spectrum centered at } f_0 \qquad (4.6) \end{aligned}$$

with $\mathbf{b}^{\mathrm{alg}}_k \overset{\mathrm{def}}{=} \mathbf{D}^{\mathrm{alg}}_{\mathbf{R}_0}\mathrm{Vec}\left(\mathbf{a}(\theta_k, f_0)\mathbf{a}^H(\theta_k, f_0) \odot \sigma_k^2\mathbf{U}_k\right)$, *and* $[\mathbf{U}_k]_{m,n} \overset{\mathrm{def}}{=} -2\pi^2\alpha^2_{m,n,k}$.

[7] Algorithm-dependent expressions of $\mathbf{D}^{\mathrm{alg}}_{\mathbf{R}_0}$ and $\mathbf{D}^{\mathrm{alg}}_{\mathbf{R}_b}$ are ordinarily deduced from perturbation calculus (see e.g., the expression (B.1) of $\mathbf{D}^{\mathrm{music}}_{\mathbf{R}_0}$ given in Appendix B).

Then, from (4.2) and (4.3), the mapping alg$(\cdot)$ gives the deviation from the asymptotic mean $\mathrm{E}(\Theta(T))$:

$$\Theta(T) - \mathrm{E}(\Theta(T)) = \mathbf{D}^{\mathrm{alg}}_{\mathbf{R}_b}\mathrm{Vec}(\delta\mathbf{R}_T) + O\left(\frac{1}{T}\right) + O(\|\delta\mathbf{R}_b\|^2). \tag{4.7}$$

We therefore have:

Result 2 *The asymptotic covariance of the estimate $\Theta(T)$ (w.r.t. to the number of snapshots and signal bandwidth) given by a narrowband SOS-based algorithm may be written as*

$$\begin{aligned}
\mathrm{Cov}(\Theta(T)) &= \frac{1}{T}\mathbf{D}^{\mathrm{alg}}_{\mathbf{R}_b}\mathbf{C}_{R_b}\left(\mathbf{D}^{\mathrm{alg}}_{\mathbf{R}_b}\right)^H + O\left(\frac{1}{T^2}\right) + O\left(\frac{1}{T}\right)O(\|\delta\mathbf{R}_b\|^2) + O(\|\delta\mathbf{R}_b\|^4) \\
&= \frac{1}{T}\mathbf{D}^{\mathrm{alg}}_{\mathbf{R}_b}(\mathbf{R}_0^* \otimes \mathbf{R}_0)\left(\mathbf{D}^{\mathrm{alg}}_{\mathbf{R}_b}\right)^H + \frac{1}{T}\mathbf{D}^{\mathrm{alg}}_{\mathbf{R}_b}(\mathbf{R}_0^* \otimes \delta\mathbf{R}_b)\left(\mathbf{D}^{\mathrm{alg}}_{\mathbf{R}_b}\right)^H + \frac{1}{T}\mathbf{D}^{\mathrm{alg}}_{\mathbf{R}_b}(\delta\mathbf{R}_b^* \otimes \mathbf{R}_0)\left(\mathbf{D}^{\mathrm{alg}}_{\mathbf{R}_b}\right)^H \\
&+ O\left(\frac{1}{T^2}\right) + O\left(\frac{1}{T}\right)O(\|\delta\mathbf{R}_b\|^2) + O(\|\delta\mathbf{R}_b\|^4)
\end{aligned} \tag{4.8}$$

with $\mathbf{C}_{R_b} = \lim_{T\to\infty} T\mathrm{Cov}(\mathrm{Vec}(\mathbf{R}_b(T)) = \lim_{T\to\infty} T\mathrm{E}(\mathrm{Vec}(\delta\mathbf{R}_T)\mathrm{Vec}^H(\delta\mathbf{R}_T)) = \mathbf{R}_b^* \otimes \mathbf{R}_b$ for independent circular complex snapshots $\mathbf{y}_t$, [3, p. 336].

These general results enable us to extend the results of [18] for symmetric spectra to the general case of non-symmetric spectra and/or offset of the centered value of the spectra w.r.t. the demodulation frequency f_0. Due to the complexity of the computations, we concentrate on the standard MUSIC algorithm and the presented results are illustrated in the cases of one source or two equipowered sources in the following subsection.

4.1 Monosource case

For the specific case of one source, the following results are proved in Appendix B:

Result 3 *The asymptotic bias (w.r.t. to the number of snapshots and signal bandwidth) is given for an arbitrary spectrum by:*

$$\begin{aligned}
\mathrm{E}(\theta_1(T)) - \theta_1 &= \frac{8\pi^2}{M\alpha_{\theta_1}}\left(\frac{f_m}{f_0}\right)\sum_{n,m=1}^{M}\alpha_{m,n,1}\frac{\mathbf{z}_n{}^T\mathbf{p}_1'}{\lambda_0} + O\left(\frac{f_\sigma^3}{f_0^3}\right) + O\left(\frac{f_m^2}{f_0^2}\right) \\
&+ O\left(\frac{f_\sigma^2 f_m}{f_0^3}\right) + O\left(\frac{1}{T}\right) \qquad \textit{for an arbitrary spectrum} \qquad (4.9) \\
&= O\left(\frac{f_\sigma^3}{f_0^3}\right) + O\left(\frac{1}{T}\right) \qquad \textit{for an arbitrary spectrum centered at } f_0 \qquad (4.10) \\
&= O\left(\frac{f_\sigma^4}{f_0^4}\right) + O\left(\frac{1}{T}\right) \qquad \textit{for a symmetric spectrum centered at } f_0 \qquad (4.11)
\end{aligned}$$

with $\mathbf{p}_1' \stackrel{\mathrm{def}}{=} \frac{d\mathbf{p}_1}{d\theta_1}$.

Result 4 *In the specific case of an arbitrary linear array and a symmetric spectrum w.r.t.* $f_0 + f_m$

$$\mathrm{E}(\phi_1(T)) - \phi_1 = \phi_1 \frac{f_m}{f_0} + O\left(\frac{f_\sigma^4}{f_0^4}\right) + O\left(\frac{1}{T}\right) \tag{4.12}$$

where ϕ_1 *denotes here the spatial parameter* $\phi_1 = \pi \sin\theta_1$*, with* θ_1 *the DOA relative to the array broadside.*

We note that the expression of the bias given for an arbitrary array and a symmetric spectrum w.r.t. f_0 in (4.11) is more accurate than the expression $\beta\left(\frac{f_\sigma^2}{f_0^2}\right) + O(\frac{1}{T})$ given in [18]. Furthermore, the numerical computation [8] of the asymptotic bias (w.r.t. the number of snapshots) satisfies $|music(\mathbf{R}_b) - \theta_1| < 10^{-6}$ for uniform linear and circular arrays (with $M \leq 20$, for all θ_1) and for a source with flat spectrum (for all b). Result 3 shows that the behavior of the estimate $\theta_1(T)$ depends critically on the symmetry and the center of the spectrum w.r.t. the demodulation frequency.

Concerning the asymptotic variance w.r.t. the number of snapshots and signal bandwidth, we prove in Appendix C the following result for an arbitrary spectrum centered on f_0:

Result 5

$$\mathrm{Var}(\theta_1^b(T)) = \mathrm{Var}(\theta_1^0(T))\left(1 + c\left(\frac{f_\sigma^2}{f_0^2}\right) + O\left(\frac{f_\sigma^4}{f_0^4}\right)\right) + O\left(\frac{1}{T^2}\right) \tag{4.13}$$

where $\mathrm{Var}(\theta_1^0(T))$ *is the classic asymptotic variance of the MUSIC algorithm for a narrowband scenario (see, e.g., [19, rel. (3.12)]) and where an expression for* c *is given in Appendix C.*

The performance degradation due to center frequency mismach is illustrated in Figs.5 and 6. These figures show the mean square error of the spatial DOA ϕ_1 estimated by the standard MUSIC algorithm: $\mathrm{MSE}(\phi_1(T)) = \mathrm{bias}^2(\phi_1(T)) + \mathrm{Var}(\phi_1(T))$ in which the bias and variance are given respectively by $\phi_1 \frac{f_m}{f_0}$ (see (4.12)) and by $\frac{1}{T}\mathbf{D}_{\mathbf{R}_b}^{\mathrm{music}}(\mathbf{R}_0^* \otimes \mathbf{R}_0 + \mathbf{R}_0^* \otimes \delta\mathbf{R}_b + \delta\mathbf{R}_b^* \otimes \mathbf{R}_0)\left(\mathbf{D}_{\mathbf{R}_b}^{\mathrm{music}}\right)^H$ (see (4.8)) where $\delta\mathbf{R}_b$ is given by (2.7) and (2.9). The principal term of this MSE may be written as

$$\mathrm{MSE}(\phi_1(T)) = \phi_1^2\left(\frac{f_m^2}{f_0^2}\right) + \left[\frac{c_0}{T} + \frac{c_1}{T}\left(\frac{f_m}{f_0}\right) + \frac{c_2}{T}\left(\frac{f_\sigma^2}{f_0^2}\right)\right], \tag{4.14}$$

in which c_0/T denotes the asymptotic variance (w.r.t. the number of snapshots) of the MUSIC algorithm acting on zero bandwidth data. *We see the key role of the frequency offset* f_m *between the centered frequency of the spectrum and the demodulation frequency* f_0*: the narrowband SOS-based algorithms are much more sensitive to frequency*

[8] We note that the relative flatness of the MUSIC localization function has prevented us from obtaining precise values of the bias due to the limited precision effects.

offset than to bandwidth. Furthermore, because the bias is constant in T, this sensitivity to f_m increases with the number of snapshots.

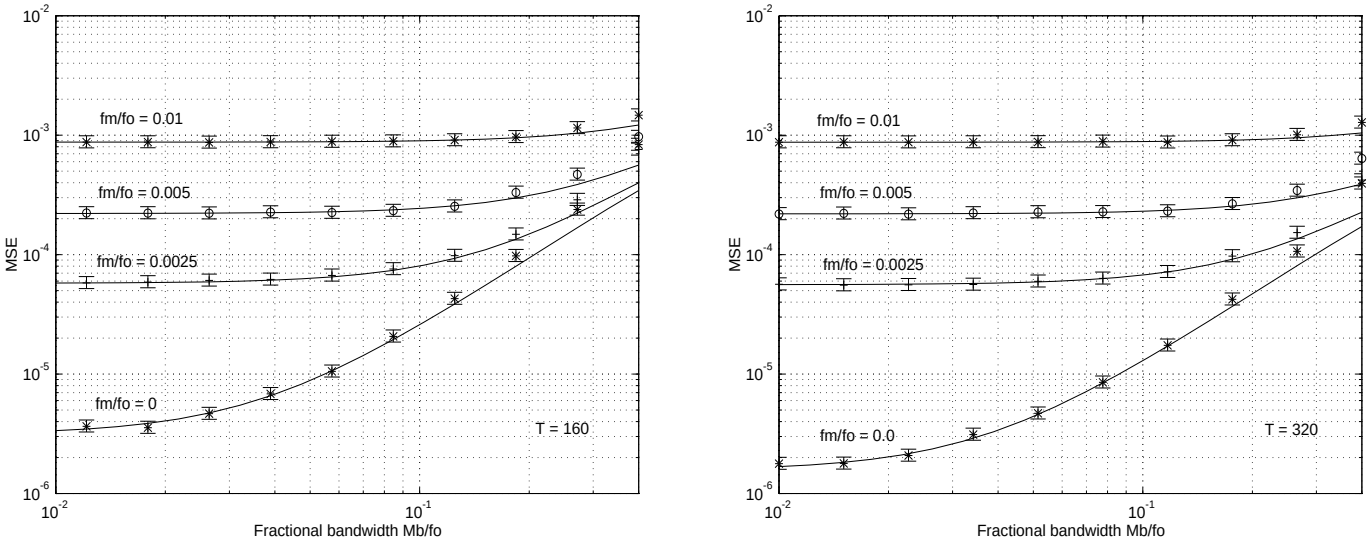

Fig.5 Analytical asymptotical (w.r.t. b and T) MSE (rel. (4.14)) and estimated MSE (1000 runs with 99% confidence interval) using the MUSIC algorithm of the spatial DOA $\phi_1 = \pi \sin\theta_1$ w.r.t. $\frac{b}{f_0}$ and $\frac{f_m}{f_0}$ for one source of centered flat spectrum of bandwidth b impinging on a uniform linear array of 5 sensors with a SNR of $20dB$ and $T = 160$ or 320.

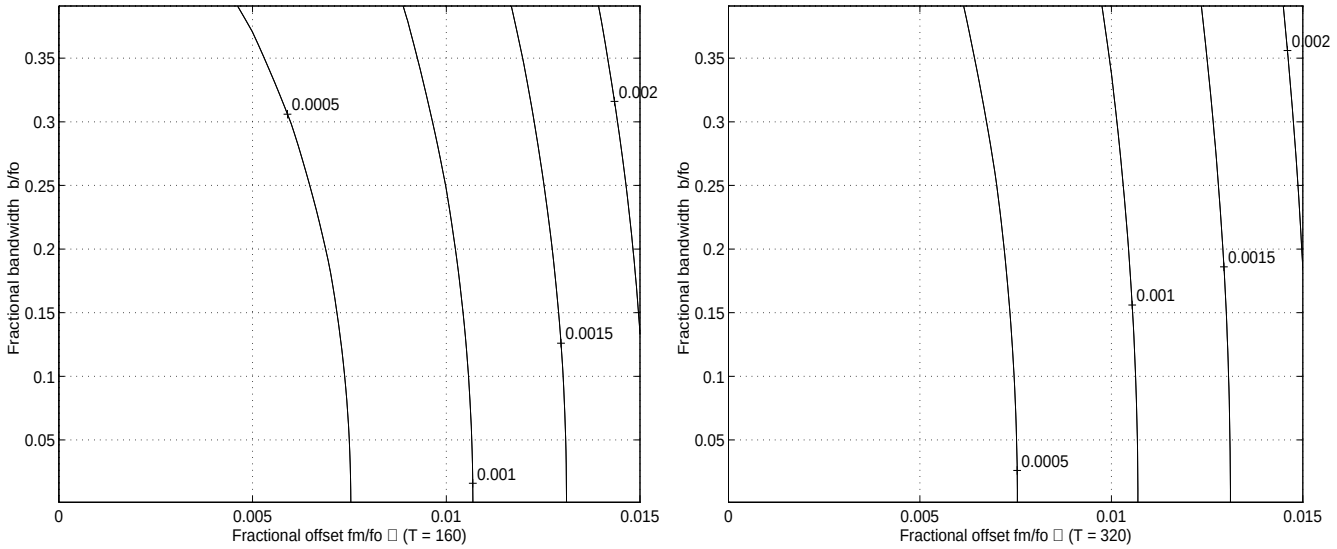

Fig.6 Constant theoretical MSE (rel.(4.14)) contours as a function of the fractional bandwidth $\frac{b}{f_0}$ and the fractional offset $\frac{f_m}{f_0}$ in the conditions of Fig.5.

4.2 Two equipowered sources case

In the case of two equipowered sources, even for symmetric spectra w.r.t. f_0, the terms $\mathbf{D}_{\mathbf{R}_0}^{\text{music}}(l,:)\text{Vec}(\delta\mathbf{R}_b)$, $l = 1, 2$, do not vanish and therefore the asymptotical bias (w.r.t. the bandwidth and the number of snapshots) is of order greater than or equal to $\frac{f_\sigma^2}{f_0^2}$. In the specific case of two symmetric spectra w.r.t. f_0, it is proved in

Appendix D that

$$\mathbf{D}_{\mathbf{R}_0}^{\text{music}}(l,:)\text{Vec}(\delta\mathbf{R}_b) = c_l\left(\frac{f_\sigma^2}{f_0^2}\right) + O\left(\frac{f_\sigma^4}{f_0^4}\right),\ l = 1,2, \tag{4.15}$$

where the expression for the constant c_l is given in Appendix D. Therefore, three asymptotic expressions of bias, w.r.t. the bandwidth and the number of snapshots, are given

$$(a)\ \mathbf{D}_{\mathbf{R}_0}^{\text{music}}(l,:)\text{Vec}(\delta\mathbf{R}_b),\ (b)\ c_l\left(\frac{f_\sigma^2}{f_0^2}\right) \text{ and } (c)\ \text{music}_l(\mathbf{R}_b) - \phi_l,\ l = 1,2.$$

in which the first two are analytical and the third is numerical.

For the parameters of Fig.7, it is shown that these three values show good agreement up to $\frac{Mb}{f_0} = 1$ and moreover, as the biases of the two sources are of opposite sign (negative for $\theta_1 = 25°$ and positive for $\theta_2 = 40°$), the estimated DOA's move further apart with increasing source bandwidth. As such, the resolution capabilities of the standard MUSIC algorithm potentially improves with increasing source bandwidth with these specific parameters. In fact, when the number of sensors increases, the estimated DOA's keep moving further apart with increasing source bandwidth, but the biases are no longer opposite. Consequently, the usual resolution capability criterion (see e.g., [10] based on a threshold equation evaluated at mid-angle $\frac{1}{2}(\theta_1 + \theta_2)$) is not appropriate for our situation. We note that these favorable properties no longer apply when the two sources have different powers.

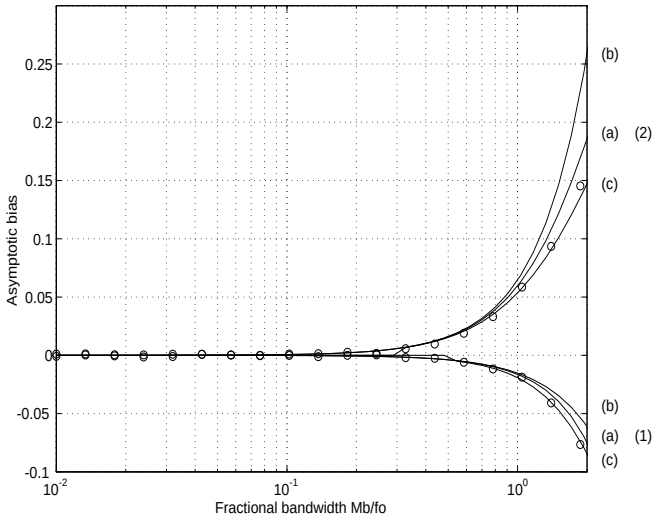

Fig.7 Asymptotic (w.r.t. b and T) (a), (b), (c) bias and estimated (dots) by Monte Carlo simulation (1000 runs) bias of the spatial DOAs $\phi_k = \pi \sin\theta_k$ for two equipowered sources of centered flat spectrum of bandwidth b, $\theta_1 = 25°$ (1), $\theta_2 = 40°$ (2) impinging on a linear array of 5 sensors, $SNR = 20dB$, $T = 160$ versus $\frac{Mb}{f_0}$.

5 Cramer-Rao lower bound

In the case of wideband sources with spectra symmetric w.r.t. the demodulation frequency f_0, it was shown in Section 4 (see rel. (4.5)), that the estimated DOA parameter given by any narrowband SOS-based algorithm is asymptotically unbiased w.r.t. the number of snapshots and signal bandwidth. Therefore, in this case, it makes sense to consider the CRB of the DOA parameter for sources of nonzero bandwidth.

Furthermore, in the case of one source, it was pointed out that the bias is negligible for all useable bandwidths. In these conditions, it is interesting to relate the CRB of the parameter θ_1 associated to a wideband and a narrowband source. In this latter case, the spatial covariance matrix (2.1) has the common expression:

$$\mathbf{R}_b = \mathbf{\Delta}_{\theta_1} \mathbf{R}_\Phi \mathbf{\Delta}_{\theta_1}^H,$$

with $\mathbf{\Delta}_{\theta_1} \stackrel{\text{def}}{=} \text{Diag}(e^{-i2\pi f_0 \tau_{1,1}}, \ldots, e^{-i2\pi f_0 \tau_{1,M}})$ and $\mathbf{R}_\Phi \stackrel{\text{def}}{=} \mathbf{R}_{s_1} + \sigma_n^2 \mathbf{I}_M$ where $\mathbf{R}_{s_1}$ is a real-valued symmetric [9] matrix thanks to the symmetry of the spectrum of the source w.r.t. the frequency f_0. Consequently, $\mathbf{R}_b$ is uniquely parameterized by $\Psi = (\theta_1, \Phi)$ where $\Phi = (\phi_{0,0}, \phi_{1,0}, \ldots, \phi_{M-1,M-1})$ with $(\phi_{i,j})_{0 \leq j \leq i \leq M-1}$ denotes the diagonal and subdiagonal of $\mathbf{R}_\Phi$. In the case of T independent circular complex Gaussian zero-mean snapshots $\mathbf{y}_t$, the CRB for the DOA parameter θ_1 alone can be obtained by following the same lines as in [2, Appendix] [10]. Therefore the CRB of the parameter θ_1 is

$$CRB_{\theta_1} = \frac{1}{2T} \left(\text{Tr}(-\mathbf{\Delta}_{\theta_1}^{'\,2} + \mathbf{\Delta}_{\theta_1}^{'} \mathbf{R}_\Phi^{-1} \mathbf{\Delta}_{\theta_1}^{'} \mathbf{R}_\Phi) \right)^{-1}, \tag{5.1}$$

where $\mathbf{\Delta}_{\theta_1}^{'} \stackrel{\text{def}}{=} -2\pi f_0 \text{Diag}(\frac{d\tau_{1,1}}{d\theta_1}, \ldots, \frac{d\tau_{1,M}}{d\theta_1})$.

We propose in the following to relate the CRB of the parameter θ_1 associated with a wideband and a narrowband source. Using the expression of CRB_{θ_1} given in (5.1), in which $\mathbf{R}_\Phi$ becomes

$$\mathbf{R}_\Phi = \left(\sigma_1^2 \mathbf{1}\mathbf{1}^T + \sigma_n^2 \mathbf{I}_M \right) + \delta \mathbf{R}_{s_1},$$

the following result is proved in Appendix E.

Result 6 *The CRB of the parameter θ_1 issued from a nonzero bandwidth source is given by*

$$CRB_{\theta_1^b} = CRB_{\theta_1^0} \left(1 + c' \left(\frac{f_\sigma^2}{f_0^2} \right) + O\left(\frac{f_\sigma^4}{f_0^4} \right) \right) \tag{5.2}$$

[9] In the specific case of a uniform linear array, $\mathbf{R}_{s_1}$ is additionally a Toeplitz matrix.

[10] We note that using the property that $\mathbf{R}_b$ is linear in the parameters Φ, another more intricate expression (requiring a projection matrix) may be obtained; see e.g., [16] with a rather elaborate proof and [1, Appendix 4.C] with a short direct proof.

where $CRB_{\theta_1^0}$ is the classic CRB given in a narrowband scenario and c' is given in Appendix E.

In the case of several sources of symmetric spectra w.r.t. f_0, the spatial covariance matrix $\mathbf{R}_b$ is parametrized by $(\theta_k)_{k=1,\ldots,K}$, σ_n^2 and the diagonal and subdiagonal of $(\mathbf{R}_{s_k})_{k=1,\ldots,K}$ (see eq. (2.4)). And this time, this parametrization is no longer unique (i.e., these parameters are not identifiable from the knowledge of $\mathbf{R}_b$ alone). To overcome this difficulty, we have to resort to side information. For example, if the normalized shape $S(f)$ (see (2.3)) of the spectra of the sources are known a priori, $\mathbf{R}_b$ is now uniquely parametrized by $\Psi = (\theta_1, \ldots, \theta_K, f_\sigma, \sigma_1^2, \ldots, \sigma_K^2, \sigma_n^2)$. In this latter case, the approach developed for one source is no longer valid [11] and we have to resign to inverting the Fisher information matrix $\mathbf{I}(\Psi)$ (see, e.g., [11, rel. (15.52)]):

$$[\mathbf{I}(\Psi)]_{k,l} = T \ \mathrm{Tr}\left(\mathbf{R}_b^{-1}\frac{\partial \mathbf{R}_b}{\partial \psi_k}\mathbf{R}_b^{-1}\frac{\partial \mathbf{R}_b}{\partial \psi_l}\right),$$

and numerically extracting the DOA's corner of $\mathbf{I}(\Psi)^{-1}$.

In the following, we illustrate the CRB of the DOA parameter in two situations. Fig.8 explores the case of one source of centered flat spectrum of bandwidth b impinging on a linear array of 5 sensors with a SNR of $20dB$ and $T = 320$, showing the mean square errors of the DOA estimated by the standard MUSIC algorithm with respect to Mb/f_0 compared with the CRB. We notice:

- a good agreement between the exact CRB (2) and the asymptotic CRB (3) $CRB_{\theta_1^0}\left(1 + c'\left(\frac{f_\sigma^2}{f_0^2}\right)\right)$ up to $\frac{Mb}{f_0} = 0.6$;
- a good agreement between the theoretical MSE and the estimated MSE given by the standard MUSIC algorithm up to $\frac{Mb}{f_0} = 1.8$;
- the asymptotic CRB (w.r.t. b) (5.2) coincides with the asymptotic MSE (w.r.t. b) (4.13) given by the standard MUSIC algorithm far all values of b.

Consequently, the standard MUSIC algorithm, which is efficient in the zero bandwidth scenario, remains efficient with increasing bandwidth up to $\frac{Mb}{f_0} = 0.6$.

[11] We note that if the normalized shape $S(f)$ and the standard deviation f_σ of the spectra are known, $\Psi = (\Theta, \Phi)$ with $\Phi \stackrel{\text{def}}{=} (\sigma_1^2, \ldots, \sigma_K^2, \sigma_n^2)$ with $\mathbf{R}_b$ linear in the parameters comprising Φ. Consequently, the approach of [1, Appendix 4.C] to directly extract a closed-form expression of the CRB for the DOA's parameter Θ alone can be used.

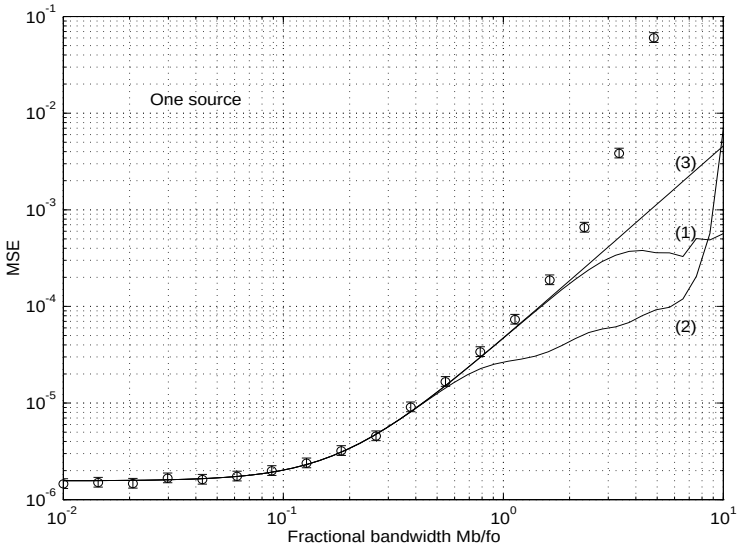

Fig.8 MSE and CRB of the spatial DOA $\phi_1 = \pi \sin\theta_1$ versus $\frac{Mb}{f_0}$,
(1) analytical asymptotical (w.r.t. b and T) MSE given by the MUSIC algorithm, (2) exact CRB_{θ_1} (5.1),
(3) asymptotic CRB_{θ_1} (w.r.t. b) (5.2) and asymptotic MSE (w.r.t. b) (4.13) given by the MUSIC algorithm,
(o) estimated (1000 runs) with 99% confidence interval (with error bars) MSE given by the MUSIC algorithm.

Fig.9 explores the case of two equipowered sources (DOA separation of 15° with $\theta_1 = 25°$) of centered flat spectrum of bandwidth b impinging on a linear array of 5 sensors with a SNR of $20dB$ and $T = 320$. We note the good agreement between the theoretical and the estimated MSE given by the standard MUSIC algorithm up to $\frac{Mb}{f_0} = 1$. Although the standard MUSIC algorithm is not efficient, this figure shows that it remains nearly efficient up to $\frac{Mb}{f_0} = 0.4$.

Fig.9 MSE and CRB of the spatial DOA $\phi_1 = \pi \sin\theta_1$ versus $\frac{Mb}{f_0}$,
(1) analytical asymptotically (w.r.t. b and T) MSE given by the MUSIC algorithm, (2) exact CRB_{θ_1},
(o) estimated (1000 runs) with 99% confidence interval (with error bars) MSE given by the MUSIC algorithm.

6 Comparison between narrowband and wideband algorithm

Naturally, a thorough comparison between narrowband and wideband algorithms would require a large quantity of scenarios (various arrays, DOA's, source spectra and SNR), and is beyond the scope of this paper. Moreover, comparing spatial covariance matrices based narrowband algorithms with cross-spectral density matrix based wideband algorithms comes up against the problem of the choice of the parameters that characterize asymptotic performance. It would seems natural to compare the respective asymptotic covariance of the estimated DOA's w.r.t. the number of snapshots. However, we note that these snapshots represent temporal samples that are generally assumed

independent in spatial covariance matrix based narrowband algorithms to simplify the performance analysis. By contrast, in the cross-spectral density matrix-based wideband algorithms, the sensor outputs are sectioned and windowed and the snapshots represent the Fourier transforms of these successive sections for the frequencies of interest. Under these conditions, the only fair setting is to compare these two approaches with the same observation interval. With the same sampling rate, this amounts to comparing them with the same number of consecutive temporal samples.

In the following, we consider the two scenarios of Section 5 where the MUSIC algorithm and the focusing algorithm by Friedlander and Weiss [9] process the same data (complex envelopes sampled at the Nyquist rate $\frac{1}{T_s} = b$). We note that, in this approach, the temporal samples are no longer independent and consequently the CRB results and the performance of the MUSIC algorithm given in Section 5 are no longer valid. However, it was shown in [8] that in the zero bandwidth scenario, the asymptotic performance of an arbitrary second-order DOA algorithm does not depend on the spectra of the sources nor on the sampling frequency if $\frac{1}{T_s} \geq b$, but on the observation time only.

Figs.10 and 11 show that the asympotic performance of the MUSIC algorithm (whose performance slightly degrades w.r.t. those of Figs.8 and 9) and of the focusing algorithm (in the conditions of Fig. 2) are equivalent up to $Mb/f_0 = 0.1$ and that the focusing algorithm slightly outperforms the MUSIC algorithm [12] for $0.1 < Mb/f_0 < 2$.

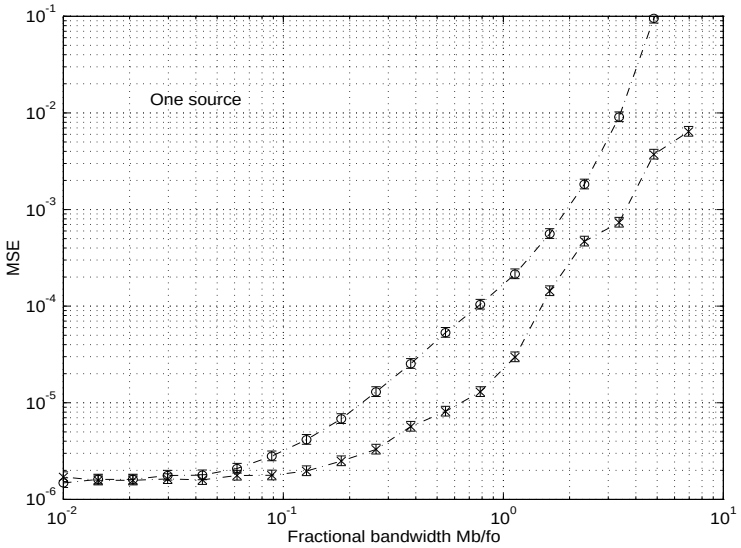

Fig.10 MSE of the spatial DOA $\phi_1 = \pi \sin\theta_1$ versus $\frac{Mb}{f_0}$ estimated (1000 runs) with 99% confidence interval by the MUSIC algorithm (o) and by a focusing algorithm (*) versus $\frac{Mb}{f_0}$

[12] Naturally, the MUSIC algorithm fails for $Mb/f_0 > 2$.

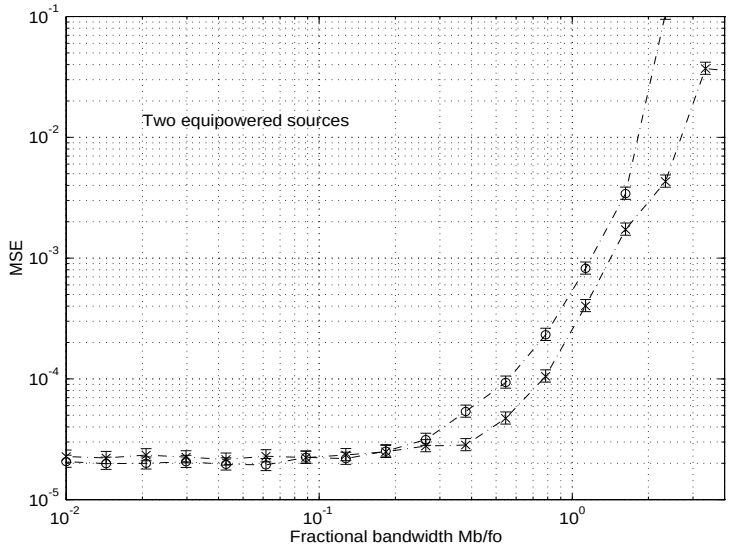

Fig.11 MSE of the spatial DOA $\phi_1 = \pi \sin\theta_1$ versus $\frac{Mb}{f_0}$ estimated (1000 runs) with 99% confidence interval by the MUSIC algorithm (o) and by a focusing algorithm (*) versus $\frac{Mb}{f_0}$

7 Conclusion

In this paper we have extended the analysis of [18] to the case of nonsymmetric spectra and/or offset of the centered value of the spectra w.r.t. the demodulation frequency f_0. We found that the behavior of the DOA estimators strongly depends on the symmetry of the source spectra w.r.t. their centered value and on the offset of this centered value w.r.t. f_0. We showed in particular that the narrowband SOS-based algorithms are much more sensitive to the frequency offset than to the bandwidth.

Considering the order detection, the Cramer-Rao bound and the comparison between narrowband and wideband algorithms, we have proved that the vague definition of narrowband scenario often given in the literature, namely, that the array aperture is much less than the inverse relative bandwidth (i.e., $\frac{Mb}{f_0} \ll 1$) is far too severe in the cases of one source or two equipowered uncorrelated sources of the same symmetric bandwidth w.r.t. the demodulation frequency.

Consequently, the narrowband DOA algorithms indeed are robust with respect to signal bandwidth, which certainly explains their popularity in practical conditions. However, questions such as spatially correlated sources and sources of different powers require further investigation.

A Proof of rels. (2.6), (2.7) and (2.8)

From (2.5), we have

$$\begin{aligned}[\mathbf{R}_{s_k}]_{m,n} &= \sigma_k^2 R\left(\frac{f_\sigma}{f_0}\alpha_{m,n,k}\right) e^{i2\pi\frac{f_m}{f_0}\alpha_{m,n,k}} \\ &= \sigma_k^2\left[1-2\pi^2\left(\frac{f_\sigma^2}{f_0^2}\right)\alpha_{m,n,k}^2+\frac{1}{6}\left(\frac{f_\sigma^3}{f_0^3}\right)\alpha_{m,n,k}^3 R'''(0)+O\left(\frac{f_\sigma^4}{f_0^4}\right)\right]\left[1+i2\pi\frac{f_m}{f_0}\alpha_{m,n,k}+O\left(\frac{f_m^2}{f_0^2}\right)\right],\end{aligned}$$

which straightforwardly gives (2.6) for an arbitrary spectrum. For an arbitrary spectrum centered at f_0, $f_m = 0$ which gives (2.7). For a symmetric spectrum w.r.t. f_0, we have $f_m = 0$ and $R'''(0) = 0$, which gives (2.8).

B Proof of rels. (4.9), (4.10), (4.11) and (4.12)

First of all, we note that the differential matrix $\mathbf{D}_{\mathbf{R}_0}^{\text{alg}}$ of the standard MUSIC algorithm deduced from perturbation calculus (see, e.g., [7]) is

$$\mathbf{D}_{\mathbf{R}_0}^{\text{music}}(l,:) = \frac{1}{\alpha_{\theta_l}}\left(\mathbf{a}_{\theta_l}^T\mathbf{\Gamma}_s^*\otimes\mathbf{a}_{\theta_l}^{'H}\mathbf{\Pi}_n + \mathbf{a}_{\theta_l}^{'T}\mathbf{\Pi}_n^*\otimes\mathbf{a}_{\theta_l}^H\mathbf{\Gamma}_s\right),\quad l=1,\ldots,K \tag{B.1}$$

where $\mathbf{\Pi}_n$ and $\mathbf{\Gamma}_s$ denote the orthogonal projection onto the noise space associated with $\mathbf{R}_0$ and the Moore-Penrose pseudoinverse $(\mathbf{R}_0-\sigma_n^2\mathbf{I}_M)^\#$, respectively, and where $\mathbf{a}_{\theta_l}\overset{\text{def}}{=}\mathbf{a}(\theta_l,f_0)$, $l=1,\ldots,K$ and α_{θ_l} is the geometrical factor $2\mathbf{a}_{\theta_l}^{'H}\mathbf{\Pi}_n\mathbf{a}_{\theta_l}^{'}$ with $\mathbf{a}_{\theta_l}^{'}\overset{\text{def}}{=}\frac{d\mathbf{a}_{\theta_l}}{d\theta_l}$. Therefore the asymptotic bias becomes

$$\begin{aligned}[\mathbf{D}_{\mathbf{R}_0}^{\text{music}}\text{Vec}(\delta\mathbf{R}_b)]_l &= \frac{2}{\alpha_{\theta_l}}\Re\left(\mathbf{a}_{\theta_l}^H\mathbf{\Gamma}_s\delta\mathbf{R}_b\mathbf{\Pi}_n\mathbf{a}_{\theta_l}^{'}\right) = \frac{2}{\alpha_{\theta_l}}\Re\left(\mathbf{a}_{\theta_l}^H\mathbf{\Gamma}_s(\mathbf{R}_b-\sigma_n^2\mathbf{I}_M)\mathbf{\Pi}_n\mathbf{a}_{\theta_l}^{'}\right) \\ &= \frac{2}{\alpha_{\theta_l}}\sum_{k=1}^K\int_{-B/2}^{+B/2}S_k(f)\Re\left(\mathbf{a}_{\theta_k}^H\mathbf{\Gamma}_s\mathbf{\Delta}_{\theta_k,f}\mathbf{a}_{\theta_k}\mathbf{a}_{\theta_k}^H\mathbf{\Delta}_{\theta_k,f}^H\mathbf{\Pi}_n\mathbf{a}_{\theta_l}^{'}\right)df\end{aligned} \tag{B.2}$$

where $\Re(.)$ denotes "the real part of" and $\mathbf{\Delta}_{\theta_k,f}\overset{\text{def}}{=}\text{Diag}(e^{-i2\pi f\tau_{k,1}},\ldots,e^{-i2\pi f\tau_{k,M}})$.

Substituting the expressions $\mathbf{\Gamma}_s = \frac{1}{M^2\sigma_1^2}\mathbf{a}_{\theta_1}\mathbf{a}_{\theta_1}^H$, $\mathbf{\Pi}_n = \mathbf{I}_M - \frac{\mathbf{a}_{\theta_1}\mathbf{a}_{\theta_1}^H}{M}$ and $\mathbf{a}_{\theta_1}^{'} = i\mathbf{\Delta}_{\theta_1}^{'}\mathbf{a}_{\theta_1}$ with $\mathbf{\Delta}_{\theta_1}^{'}\overset{\text{def}}{=}\text{Diag}(-2\pi f_0\tau_{1,1}^{'},\ldots,-2\pi f_0\tau_{1,M}^{'})$ in (B.2) we get

$$[\mathbf{D}_{\mathbf{R}_0}^{\text{music}}\text{Vec}(\delta\mathbf{R}_b)]_1 = -\frac{2}{M\alpha_{\theta_1}\sigma_1^2}\int_{-B/2}^{+B/2}S_1(f)\Im\left(\mathbf{a}_{\theta_1}^H\mathbf{\Delta}_{\theta_1,f}\mathbf{a}_{\theta_1}\mathbf{a}_{\theta_1}^H\mathbf{\Delta}_{\theta_1,-f}(\mathbf{I}_M-\frac{\mathbf{a}_{\theta_1}\mathbf{a}_{\theta_1}^H}{M})\mathbf{\Delta}_{\theta_1}^{'}\mathbf{a}_{\theta_1}\right)df.$$

Because $\mathbf{a}_{\theta 1}^H\mathbf{\Delta}_{\theta_1,f}\mathbf{a}_{\theta_1}=\sum_{m=1}^M e^{-i2\pi f\tau_{1,m}}$ and $\mathbf{a}_{\theta_1}^H\mathbf{\Delta}_{\theta_1,-f}\mathbf{\Delta}_{\theta_1}^{'}\mathbf{a}_{\theta_1}=-\sum_{n=1}^M(2\pi f_0\tau_{1,n}^{'})e^{i2\pi f\tau_{1,n}}$, the asymptotic bias becomes, after some algebra,

$$[\mathbf{D}_{\mathbf{R}_0}^{\text{music}}\text{Vec}(\delta\mathbf{R}_b)]_1 = \frac{2}{M\alpha_{\theta_1}\sigma_1^2}\sum_{n=1}^M 2\pi f_0\tau_{1,n}^{'}\Im\left(\sum_{m=1}^M\int_{-B/2}^{+B/2}S_1(f)e^{i2\pi f(\tau_{1,n}-\tau_{1,m})}df\right)$$

$$
\begin{aligned}
- & \frac{2}{M^2\alpha_{\theta_1}\sigma_1^2}\sum_{n=1}^{M} 2\pi f_0 \tau_{1,n}^{'} \Im\left(\sum_{m,l=1}^{M}\int_{-B/2}^{+B/2} S_1(f) e^{i2\pi f(\tau_{1,l}-\tau_{1,m})} df\right) \\
= & \frac{2}{M\alpha_{\theta_1}}\sum_{n=1}^{M} 2\pi f_0 \tau_{1,n}^{'} \Im\left(\sum_{m=1}^{M} R\left(f_\sigma(\tau_{1,n}-\tau_{1,m})\right) e^{i2\pi f_m(\tau_{1,n}-\tau_{1,m})}\right) \\
- & \frac{2}{M^2\alpha_{\theta_1}}\sum_{n=1}^{M} 2\pi f_0 \tau_{1,n}^{'} \Im\left(\sum_{m,l=1}^{M} R\left(f_\sigma(\tau_{1,l}-\tau_{1,m})\right) e^{i2\pi f_m(\tau_{1,l}-\tau_{1,m})}\right).
\end{aligned}
$$

The normalized correlation $R(t)$ satisfies $R(t) = 1 - 2\pi^2 t^2 + O(t^3)$ which proves (4.9) in case of an arbitrary spectrum and (4.10) in case of an arbitrary spectrum centered at f_0. For a symmetric spectrum w.r.t. f_0, $R(t)$ is real and symmetric. Consequently, the asymptotic bias is vanishing and thanks to the expression (2.9) of $\delta\mathbf{R}_b$, (4.11) is proved.

In the specific case of an arbitrary linear array and of a symmetric spectrum w.r.t. $f_0 + f_m$, $\mathbf{R}_b$ can be written as $\mathbf{R}_b = \sigma_1^2 \mathbf{a}(\theta_1, f_0+f_m)\mathbf{a}^H(\theta_1, f_0+f_m) \odot \mathbf{R}_{s_1}^{'} + \sigma_n^2 \mathbf{I}_M$ where $\mathbf{R}_{s_1}^{'}$ is symmetric and real. Therefore $\mathbf{R}_b$ may be considered as a perturbation of $\mathbf{R}_0^{'} \stackrel{\text{def}}{=} \sigma_1^2 \mathbf{a}(\theta_1, f_0+f_m)\mathbf{a}^H(\theta_1, f_0+f_m)$: $\mathbf{R}_b = \mathbf{R}_0^{'} + \delta\mathbf{R}_b^{'}$ and a first-order perturbation analysis of a narrowband SOS-based algorithm estimating ϕ_1 acting on $\mathbf{R}_b$ evaluated at point $\mathbf{R}_0^{'}$ gives

$$
\begin{aligned}
\text{alg}(\mathbf{R}_b) &= \text{alg}(\mathbf{R}_0^{'}) + (D^{\text{alg}}_{\mathbf{R}_0^{'}}, \delta\mathbf{R}_b^{'}) + O(\|\delta\mathbf{R}_b^{'}\|^2) \\
&= \phi_1 \frac{f_0+f_m}{f_0} + \mathbf{D}^{\text{alg}}_{\mathbf{R}_0^{'}} \text{Vec}(\delta\mathbf{R}_b^{'}) + O(\|\delta\mathbf{R}_b^{'}\|^2). \qquad \text{(B.3)}
\end{aligned}
$$

Following the steps of the proof of (4.11) gives the proof of (4.12). We note that (4.12) can also be derived from (4.9) applied to ϕ_1 from straightforward but tedious calculus.

C Proof of rel. (4.13)

From result 2 where $\mathbf{D}^{\text{music}}_{\mathbf{R}_b}$ is replaced by $\mathbf{D}^{\text{music}}_{\mathbf{R}_0}$ because $\mathbf{D}^{\text{music}}_{\mathbf{R}_b} = \mathbf{D}^{\text{music}}_{\mathbf{R}_0} + O(\|\delta\mathbf{R}_b\|^2)$, $\text{Var}(\theta_1^b(T))$ is given by

$$
\begin{aligned}
\text{Var}(\theta_1^b(T)) &= \text{Var}(\theta_1^0(T)) + \frac{1}{T}\left(\frac{f_\sigma^2}{f_0^2}\right) \mathbf{D}^{\text{music}}_{\mathbf{R}_0} \left(\mathbf{R}_0^* \otimes (\sigma_1^2 \mathbf{a}_{\theta_1}^H \mathbf{a}_{\theta_1} \odot \mathbf{U}_1) + (\sigma_1^2 \mathbf{a}_{\theta_1}^H \mathbf{a}_{\theta_1} \odot \mathbf{U}_1)^* \otimes \mathbf{R}_0\right) \left(\mathbf{D}^{\text{music}}_{\mathbf{R}_0}\right)^H \\
&+ O\left(\frac{1}{T^2}\right) + O\left(\frac{f_\sigma^4}{f_0^4}\right).
\end{aligned}
$$

where from (B.1), $\mathbf{D}^{\text{music}}_{\mathbf{R}_0} = \frac{1}{\alpha_{\theta_1}}\left(\mathbf{a}_{\theta_1}^T \mathbf{\Gamma}_s^* \otimes \mathbf{a}_{\theta_1}^{'H} \mathbf{\Pi}_n + \mathbf{a}_{\theta_1}^{'T} \mathbf{\Pi}_n^* \otimes \mathbf{a}_{\theta_1}^H \mathbf{\Gamma}_s\right)$ with $\alpha_{\theta_1} = 2\left(\|\mathbf{a}_{\theta_1}^{'}\|^2 - \frac{|\mathbf{a}_{\theta_1}^H \mathbf{a}_{\theta_1}^{'}|^2}{M}\right)$. (4.13) is proved after some straightforward but tedious algebraic manipulations, where c becomes

$$
c = \frac{2}{\alpha_{\theta_1}}\frac{\sigma_1^2}{\sigma_n^2}\left(\mathbf{d}_{\theta_1}^H \mathbf{U}_1 \mathbf{d}_{\theta_1} + \frac{2}{M}\Im[(\mathbf{a}_{\theta_1}^{'H}\mathbf{a}_{\theta_1})(\mathbf{d}_{\theta_1}^H \mathbf{U}_1 \mathbf{1})] + \frac{1}{M}\frac{\sigma_1^2 |\mathbf{a}_{\theta_1}^H \mathbf{a}_{\theta_1}^{'}|^2 + \sigma_n^2 \|\mathbf{a}_{\theta_1}^{'}\|^2}{\sigma_n^2 + M\sigma_1^2}(\mathbf{1}^T \mathbf{U}_1 \mathbf{1})\right) \qquad \text{(C.1)}
$$

thanks to the identities $\mathbf{x}^T(\mathbf{A}\odot\mathbf{B})\mathbf{y} = \mathrm{Tr}[\mathrm{Diag}(\mathbf{x})\mathbf{A}\mathrm{Diag}(\mathbf{y})\mathbf{B}^T]$ with $\mathrm{Diag}(\mathbf{a}_{\theta_1}) = \mathbf{\Delta}_{\theta_1}$, $\mathrm{Diag}(\mathbf{a}'_{\theta_1}) = i\mathbf{\Delta}'_{\theta_1}\mathbf{\Delta}_{\theta_1}$, $\mathbf{\Delta}^H_{\theta_1}\mathbf{a}_{\theta_1} = \mathbf{1}$ and $\mathbf{d}_{\theta_1} \stackrel{\text{def}}{=} \mathbf{\Delta}'_{\theta_1}\mathbf{1}$.

D Proof of rel. (4.15)

Using the expression of $\delta\mathbf{R}_b$ deduced from (2.8), viz.,

$$\delta\mathbf{R}_b = \left(\frac{f_\sigma^2}{f_0^2}\right)\sum_{k=1}^{2}(\mathbf{a}_{\theta_k}\mathbf{a}_{\theta_k}^H \odot \sigma_k^2\mathbf{U}_k) + O\left(\frac{f_\sigma^4}{f_0^4}\right),$$

expression (4.15) follows where the constant c_1 and c_2 are given by

$$c_l = \frac{1}{\alpha_{\theta_l}}\left(\mathbf{a}_{\theta_l}^T\mathbf{\Gamma}_s^*\otimes\mathbf{a}_{\theta_l}^{'H}\mathbf{\Pi}_n + \mathbf{a}_{\theta_l}^{'T}\mathbf{\Pi}_n^*\otimes\mathbf{a}_{\theta_l}^H\mathbf{\Gamma}_s\right)\sum_{k=1}^{2}(\mathbf{a}_{\theta_k}^*\otimes\mathbf{a}_{\theta_k})\odot\sigma^2\mathrm{Vec}(\mathbf{U}_k)\quad l=1,2,$$

in which $\sigma \stackrel{\text{def}}{=} \sigma_1 = \sigma_2$ and where $\mathbf{\Gamma}_s$ and $\mathbf{\Pi}_n$ are given respectively by

$$\begin{aligned}\mathbf{\Gamma}_s &= \frac{1}{M^2\sigma^2(1-|\beta|^2)^2}\left((1+|\beta|^2)(\mathbf{a}_{\theta_1}\mathbf{a}_{\theta_1}^H+\mathbf{a}_{\theta_2}\mathbf{a}_{\theta_2}^H) - 2\beta^*\mathbf{a}_{\theta_2}\mathbf{a}_{\theta_1}^H - 2\beta\mathbf{a}_{\theta_1}\mathbf{a}_{\theta_2}^H\right)\\ \mathbf{\Pi}_n &= \mathbf{I}_M - \frac{1}{M(1-|\beta|^2)}\left(\mathbf{a}_{\theta_1}\mathbf{a}_{\theta_1}^H+\mathbf{a}_{\theta_2}\mathbf{a}_{\theta_2}^H-\beta^*\mathbf{a}_{\theta_2}\mathbf{a}_{\theta_1}^H-\beta\mathbf{a}_{\theta_1}\mathbf{a}_{\theta_2}^H\right)\end{aligned}$$

with $\beta \stackrel{\text{def}}{=} \frac{\mathbf{a}_{\theta_1}^H\mathbf{a}_{\theta_2}}{\|\mathbf{a}_\theta\|^2}$.

E Proof of rel. (5.2)

Using $\mathbf{R}_\Phi = \sigma_1^2\mathbf{1}\mathbf{1}^T + (\sigma_n^2\mathbf{I}_M + \delta\mathbf{R}_{s_1})$ with

$$(\sigma_n^2\mathbf{I}_M + \delta\mathbf{R}_{s_1})^{-1} = \frac{1}{\sigma_n^2}\mathbf{I}_M - \frac{1}{\sigma_n^4}\delta\mathbf{R}_{s_1} + O(\delta\mathbf{R}_{s_1}^2),$$

the matrix inversion lemma (see, e.g., [11, p.571]) gives, after some algebraic manipulations,

$$\begin{aligned}\mathbf{R}_\Phi^{-1} &= \left(\frac{1}{\sigma_n^2}\mathbf{I}_M - \frac{1}{\sigma_n^4}\delta\mathbf{R}_{s_1}\right) - \left(\frac{1}{\sigma_n^2}\mathbf{I}_M - \frac{1}{\sigma_n^4}\delta\mathbf{R}_{s_1}\right)\\ &\quad\left(\frac{\sigma_n^2\sigma_1^2}{M\sigma_1^2+\sigma_n^2}\mathbf{1}\mathbf{1}^T + \frac{\sigma_1^4}{(M\sigma_1^2+\sigma_n^2)^2}\mathbf{1}\mathbf{1}^T\delta\mathbf{R}_{s_1}\mathbf{1}\mathbf{1}^T + O(\delta\mathbf{R}_{s_1}^2)\right)\left(\frac{1}{\sigma_n^2}\mathbf{I}_M - \frac{1}{\sigma_n^4}\delta\mathbf{R}_{s_1}\right) + O(\delta\mathbf{R}_{s_1}^2)\\ &= \frac{1}{\sigma_n^2}\mathbf{I}_M - \frac{\sigma_1^2}{\sigma_n^2(M\sigma_1^2+\sigma_n^2)}\mathbf{1}\mathbf{1}^T + a(\delta\mathbf{R}_{s_1}) + O(\delta\mathbf{R}_{s_1}^2)\end{aligned}$$

where $a(\delta\mathbf{R}_{s_1})$ is the following linear expression of $\delta\mathbf{R}_{s_1}$:

$$\begin{aligned}a(\delta\mathbf{R}_{s_1}) &\stackrel{\text{def}}{=} -\frac{1}{\sigma_n^4}\delta\mathbf{R}_{s_1} + \frac{\sigma_1^2}{\sigma_n^4(M\sigma_1^2+\sigma_n^2)}(\delta\mathbf{R}_{s_1}\mathbf{1}\mathbf{1}^T + \mathbf{1}\mathbf{1}^T\delta\mathbf{R}_{s_1}) - \frac{\sigma_1^4}{\sigma_n^4(M\sigma_1^2+\sigma_n^2)^2}\mathbf{1}\mathbf{1}^T\delta\mathbf{R}_{s_1}\mathbf{1}\mathbf{1}^T\\ &= \sigma_1^2\left(\frac{f_\sigma^2}{f_0^2}\right)\left(-\frac{1}{\sigma_n^4}\mathbf{U}_1 + \frac{\sigma_1^2}{\sigma_n^4(M\sigma_1^2+\sigma_n^2)}(\mathbf{U}_1\mathbf{1}\mathbf{1}^T+\mathbf{1}\mathbf{1}^T\mathbf{U}_1) - \frac{\sigma_1^4}{\sigma_n^4(M\sigma_1^2+\sigma_n^2)^2}(\mathbf{1}\mathbf{1}^T\mathbf{U}_1\mathbf{1}\mathbf{1}^T)\right)\\ &+ O\left(\frac{f_\sigma^4}{f_0^4}\right) = \sigma_1^2\left(\frac{f_\sigma^2}{f_0^2}\right)\bar{\mathbf{R}}_{s_1} + O\left(\frac{f_\sigma^4}{f_0^4}\right)\end{aligned}$$

with $\bar{\mathbf{R}}_{s_1} \stackrel{\text{def}}{=} -\frac{1}{\sigma_1^4}\mathbf{U}_1 + \frac{\sigma_1^2}{\sigma_n^4(M\sigma_1^2+\sigma_n^2)}(\mathbf{U}_1\mathbf{1}\mathbf{1}^T + \mathbf{1}\mathbf{1}^T\mathbf{U}_1) - \frac{\sigma_1^4}{\sigma_n^4(M\sigma_1^2+\sigma_n^2)^2}(\mathbf{1}\mathbf{1}^T\mathbf{U}_1\mathbf{1}\mathbf{1}^T)$, and where $\mathbf{U}_1$ is defined in Result 1. To derive the CRB of the parameter θ_1, we must consider matrices $\mathbf{\Delta}_{\theta_1}^{'}\mathbf{R}_\Phi^{-1}\mathbf{\Delta}_{\theta_1}^{'}\mathbf{R}_\Phi$ and $\mathbf{\Delta}_{\theta_1}^{'\,2}$ (see (5.1)). Substituting the expressions of $\mathbf{R}_\Phi$ and $\mathbf{R}_\Phi^{-1}$, we get after some tedious algebraic manipulations

$$-\mathrm{Tr}(\mathbf{\Delta}_{\theta_1}^{'\,2}) + \mathrm{Tr}(\mathbf{\Delta}_{\theta_1}^{'}\mathbf{R}_\Phi^{-1}\mathbf{\Delta}_{\theta_1}^{'}\mathbf{R}_\Phi) = \frac{\left(\frac{\sigma_1^4}{\sigma_n^4}\right)\left(\|\mathbf{a}_{\theta_1}\|^2\|\mathbf{a}_{\theta_1}'\|^2 - |\mathbf{a}_{\theta_1}^{'H}\mathbf{a}_{\theta_1}|^2\right)}{1+M\left(\frac{\sigma_1^2}{\sigma_n^2}\right)}\left(1 - c'\left(\frac{f_\sigma^2}{f_0^2}\right) + O\left(\frac{f_\sigma^4}{f_0^4}\right)\right)$$

with

$$c' = \frac{1}{\|\mathbf{a}_{\theta_1}\|^2\|\mathbf{a}_{\theta_1}'\|^2 - |\mathbf{a}_{\theta_1}^{'H}\mathbf{a}_{\theta_1}|^2} = \left[\beta_1\mathbf{d}_{\theta_1}^T\mathbf{U}_1\mathbf{d}_{\theta_1} + \beta_2\mathbf{1}^T\mathbf{U}_1\mathbf{1} - 2\mathbf{d}_{\theta_1}^T\mathbf{\Delta}_{\theta_1}^{'}\mathbf{U}_1\mathbf{1} + \beta_3\Im(\mathbf{d}_{\theta_1}^T\mathbf{U}_1\mathbf{1}\mathbf{a}_{\theta_1}^{'H}\mathbf{a}_{\theta_1})\right]$$

where

$$\beta_1 \stackrel{\text{def}}{=} \frac{M\sigma_1^2+2\sigma_n^2}{\sigma_n^2}, \quad \beta_2 \stackrel{\text{def}}{=} \frac{\sigma_1^2\sigma_n^2\|\mathbf{a}_{\theta_1}'\|^2 + \sigma_1^4|\mathbf{a}_{\theta_1}^{'H}\mathbf{a}_{\theta_1}|^2}{\sigma_n^2(M\sigma_1^2+\sigma_n^2)} \quad \text{and} \quad \beta_3 \stackrel{\text{def}}{=} 2\frac{\sigma_1^2}{\sigma_n^2}.$$

Consequently applying (5.1), result 6 is proved if we note that the CRB given in the narrowband scenario (see e.g., [15, rel. (17)]) becomes with our notations,

$$CRB_{\theta_1^0} = \frac{1}{2T}\frac{1+M\left(\frac{\sigma_1^2}{\sigma_n^2}\right)}{\left(\frac{\sigma_1^4}{\sigma_n^4}\right)\left(\left(\|\mathbf{a}_{\theta_1}^{'}\|^2\|\mathbf{a}_{\theta_1}\|^2 - |\mathbf{a}_{\theta_1}^H\mathbf{a}_{\theta_1}^{'}|^2\right)\right.}.$$

References

[1] M. Bengtsson, *Antenna array signal processing for high rank data models*, PhD thesis, Royal Institute of technology, Stockholm, Sweden, December 1999. TRITA-S3-SB-9938.

[2] O. Besson, P. Stoica, "Decoupled estimation of DOA and angular spread for spatially distributed source," *IEEE Trans. on Signal Processing*, vol. 48, no. 7, pp. 1872-1882, June 2000.

[3] D.R. Brillinger, *Times series, data analysis and theory.* Expanded Edition, Holden-Day, Inc., 1980.

[4] K. Buckley, "Spatial/spectral filtering with linearly constrained minimum variance beamformers," *IEEE Trans. Acoust. Speech and Signal Process.*, vol. 35, no. 3, pp. 249-266, March 1987.

[5] K. Buckley, L. Griffiths, "Broadband signal-subspace spatial-spectrum (BASS-ALE) estimation for sensor array processing," *IEEE Trans. Acoust. Speech and Signal Process.*, vol. 36, no. 7, pp. 953-964, July 1988.

[6] P.E. Caines, *Linear stochastic systems*, Wiley series in probability and mathematical statistics, 1988.

[7] J.F. Cardoso, E. Moulines, "Asymptotic performance analysis of direction-finding algorithms based on fourth-order cumulants," *IEEE Trans. Signal Processing*, vol. 43, no. 1, pp. 214-224, Jan. 1995.

[8] J.P. Delmas, "Asymptotic performance of second-order algorithms," *IEEE Trans. Signal Processing*, vol. 50, no. 1, pp. 49-57, January 2002.

[9] B. Friedlander, A.J. Weiss, "Direction finding for wide-band signals using an interpolated array," *IEEE Trans. on Signal Processing*, vol. 41, no. 4, pp. 1618-1634, April 1993.

[10] M. Kaveh, A.J. Barabell, "The statistical performance of MUSIC and the minimum-norm algorithms in resolving plane waves in noise," *IEEE Trans. Acoust. Speech, Signal Processing*, vol. 34, no. 2, pp. 331-341, April 1986.

[11] S.M. Kay, *Fundamentals of statistical signal processing, Estimation theory*, New York: Prentice Hall, 1993.

[12] J. Krolick, *Focused wideband array processing for spatial estimation* in Advances in spectrum analysis and array processing, vol. II, Simon Haykin, Editor, Prentice Hall, 1991.

[13] A.P. Liavas, P.A. Regalia and J.P. Delmas, "Blind channel approximation: Effective channel order determination," *IEEE Trans. Signal Processing*, vol. 47, no. 12, pp. 3336-3344, Dec. 1999.

[14] A.P. Liavas, P.A. Regalia, "On the behavior of information theoretical criteria for model order selection," *IEEE Trans. Signal Processing*, vol. 49, no. 8, pp. 1689-1695, Aug. 2001.

[15] B. Ottersten, M. Viberg and T. Kailath, "Analysis of subspace fitting and ML techniques for parameter estimation from sensor array data," *IEEE Trans. on Signal Processing*, vol. 40, no. 3, pp. 590-599, March 1992

[16] B. Ottersten, P. Stoica and R. Roy, "Covariance matching estimation techniques for array signal processing," *Digital Signal Processing*, vol. 8, pp. 185-210, 1998.

[17] S.V. Schell, W.A. Gardner, "High-resolution direction finding," *in Handbook of Statistics 10, Signal Processing and its Applications, edited by N.K. Bose and C.R. Rao*, Elsevier Science, 1994.

[18] J. Sorelius, R.L. Moses, T. Söderström and A.L. Swindlehurst, "Effects of nonzero bandwidth on direction of arrival estimators in array processing," *IEE Proc. Radar, Sonar Navig.*, vol. 145, no. 6, pp. 317-324, December 1998.

[19] P. Stoica, A. Nehorai, "MUSIC, Maximum likelihood, and Cramer-Rao Bound," *IEEE Trans. Acoust. Speech, Signal Processing*, vol. 37, no. 5, pp. 720-741, May 1989.

[20] H. Wang, M. Kaveh, "Coherent signal subspace processing for the detection and estimation of angles of arrival of multiple wide-band sources," *IEEE Trans. Acoust., Speech, Signal Processing*, vol. 33, no. 4, pp. 823-831, Aug. 1985.

[21] W. Xu, M. Kaveh, "Analysis of the performance and sensitivity of eigendecomposition-based detectors," *IEEE Trans. on Signal Processing*, vol. 43, no. 6, pp. 1413-1426, June 1995.

[22] M. Zatman, "How narrow is narrowband," *IEE Proc. Radar, Sonar Navig.*, vol. 145, no. 2, pp. 85-91, April 1998.